Agricultural Robot for Radicchio Harvesting

Mario M. Foglia
Department of Mechanical and Management Engineering
Politecnico of Bari
Viale Japigia 182
Bari 70126, Italy
e-mail: mm.foglia@poliba.it

Giulio Reina
Department of Innovation Engineering
University of Lecce
via per Arnesano
Lecce 73100, Italy
e-mail: giulio.reina@unile.it

Received 5 December 2005; accepted 25 May 2006

In the last few years, robotics has been increasingly adopted in agriculture to improve productivity and efficiency. This paper presents recent and current work at the Politecnico of Bari, in collaboration with the University of Lecce, in the field of agriculture robotics. A cost effective robotic arm is introduced for the harvesting of radicchio, which employs visual localization of the plants in the field. The proposed harvester is composed of a double four-bar linkage manipulator and a special gripper, which fulfills the requirement for a plant cut approximately 10 mm underground. Both manipulator and end-effector are pneumatically actuated, and the gripper works with flexible pneumatic muscles. The system employs computer vision to localize the plants in the field based on intelligent color filtering and morphological operations; we call this algorithm the radicchio visual localization (RVL). Details are provided for the functional and executive design of the robotic arm and its control system. Experimental results are discussed; obtained with a prototype operating in a laboratory testbed showing the feasibility of the system in localizing and harvesting radicchio plants. The performance of the RVL is analyzed in terms of accuracy, robustness to noises, and variations in lighting, and is also validated in field experiments. © 2006 Wiley Periodicals, Inc.

Journal of Field Robotics 23(6/7), 363–377 (2006) © 2006 Wiley Periodicals, Inc.
Published online in Wiley InterScience (www.interscience.wiley.com). • DOI: 10.1002/rob.20131

1. INTRODUCTION

Agricultural automation has become a major issue in recent years. Most of the efforts in this extensive research area have been devoted to fresh market fruit and vegetable harvesting tasks, which are generally, time consuming, tiring, and particularly demanding. For many crops, harvest labor accounts for as much as one-half to two-thirds of the total labor costs. Moreover, harvesting is expected to be automated due to a decrease in the farmer population (Burks *et al.*, 2005).

Extensive research has been conducted in applying robots to a variety of agricultural harvests; Apples, asparagus, citrus, cucumbers, grapes, lettuce, tomatoes, melons, watermelons, oranges, and strawberries. Some notable examples of agricultural robotic systems can be found in literature (Amaha, Shono, & Takakura, 1989; Arima, Kondo, & Monta, 2004; Brown, 2002; Edan, Rogozin, Flash, & Miles, 2000; Hannan & Burks, 2004; Harrell, Adsit, Munilla, & Slaughter, 1990; Kawamura & Namikawa, 1989; Kanemitsu, Yamamoto, Shibano, Goto, & Suzuki, 1993; Monta, Kondo, & Shibano, 1995; Murakami, Inoue, & Otsuka, 1995; Peterson & Wolford, 2003; Sitthichareonchai & Sevila, 1989; Van Henten *et al.*, 2002).

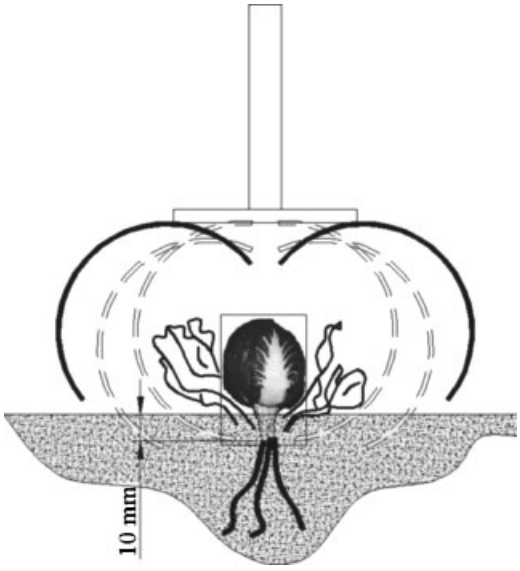

Figure 1. Radicchio requires accurate stem cutting 10 mm underground.

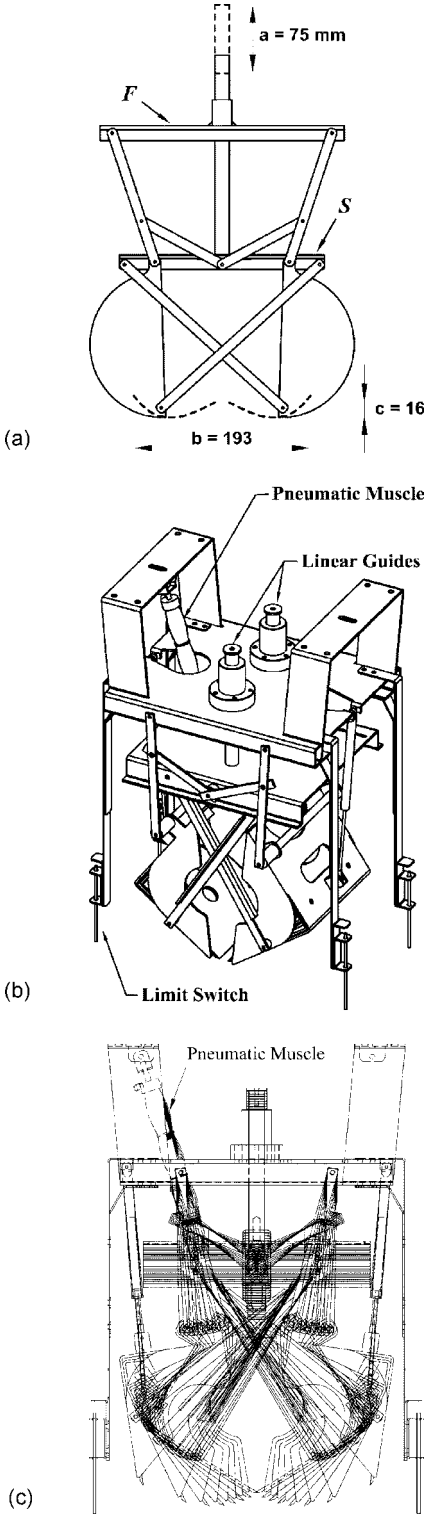

Figure 2. The two-finger gripper (a), the mechanical design (b), and the cutting sequence (c).

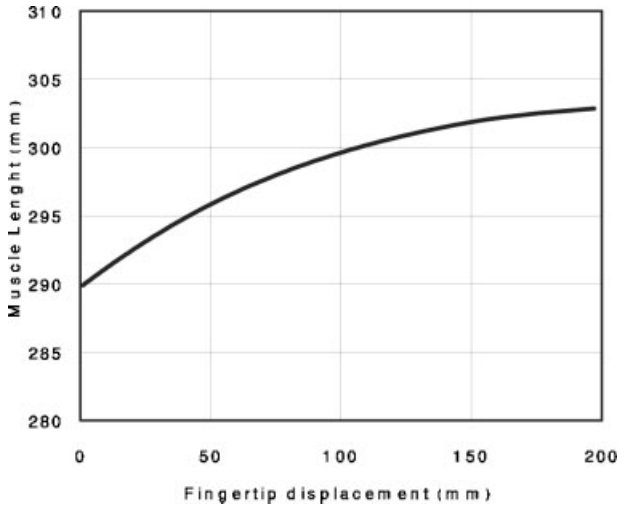

Figure 3. Fingertip displacement as function of the pneumatic muscle length for the radicchio gripper.

Specific work on robotic end-effectors for agricultural operations, such as harvesting, spraying, transplanting, and berry thinning has been developed in recent years (Kondo *et al.*, 1992; Ling *et al.*, 2004; Mattiazzo, Mauro, Raparelli, & Velardocchia, 1995; Monta *et al.*, 1992; Monta *et al.*, 1998). They are important components in the development of agricultural robotics because they directly handle plants and can influence the market value of the product.

Computer vision has also been widely employed in agriculture for developing visual guidance systems (Benson, Reid, & Zhang, 2003; Pilarski *et al.*, 1999; Slaughter, Chen, & Curley, 1999), for fruit recognition on trees (Cerruto & Schillaci, 1994; Peterson, Whiting, & Wolford, 2003; Slaughter & Harrel, 1987), grade judgment of fruits (Nagata & Cao, 1998) and for weed control (Åstrand & Baerveldt, 2002; Doeney, Gilles, & Slaughter, 2003; Jeon, Tian, & Grift, 2005). Specific research on vision-based harvesting of asparagus can be found in Humburg & Reid (1992), of melons in Cardenas-Weber, Hetzroni, & Miles (1991) and Dobrusin, Edan, Grinshpun, Peiper, & Hetzroni (1992), and of tomatoes in (Chi & Ling, 2004; Kondo, Nishitsuji, Ling, & Ting, 1996).

This paper describes current work at the Politecnico of Bari, in collaboration with the University of Lecce, in the area of robotic harvesting of fresh market vegetables. An agricultural robot for the harvesting of red radicchio is presented based on a double four-bar linkage architecture and a specialized gripper. The radicchio, widely grown in Italy, is a red broad leaf heading form of chicory and requires a stem cutting approximately 10 mm underground

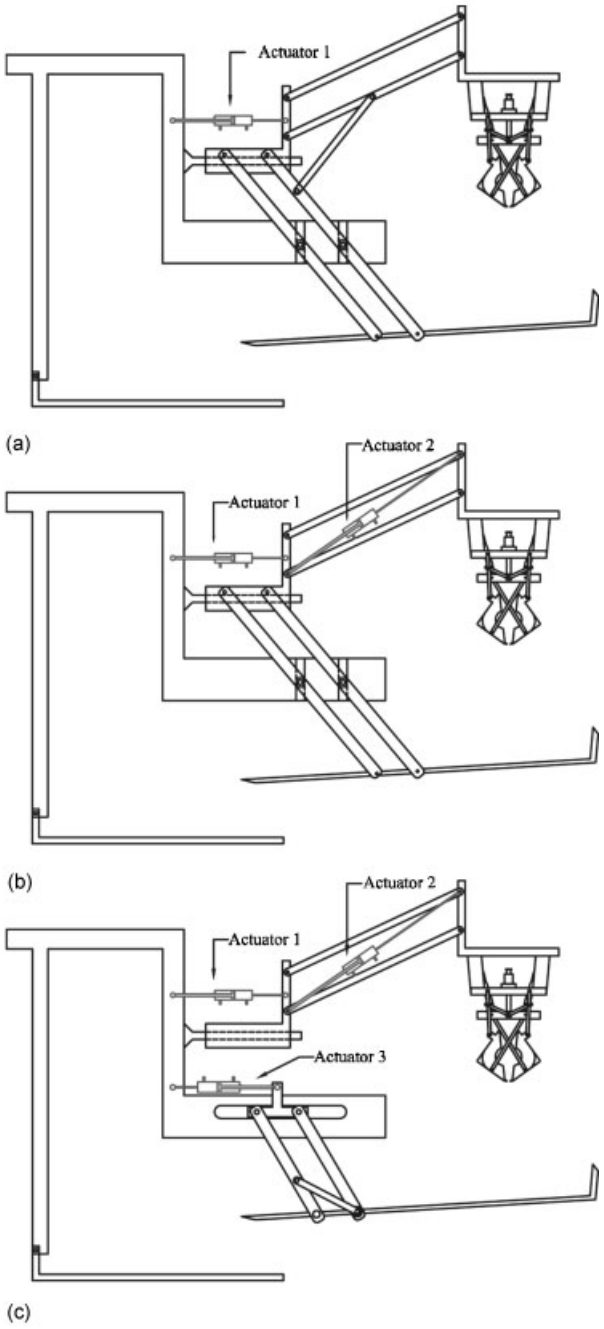

Figure 4. Four bar-based manipulator employing: One (a), two (b), and three actuators (c).

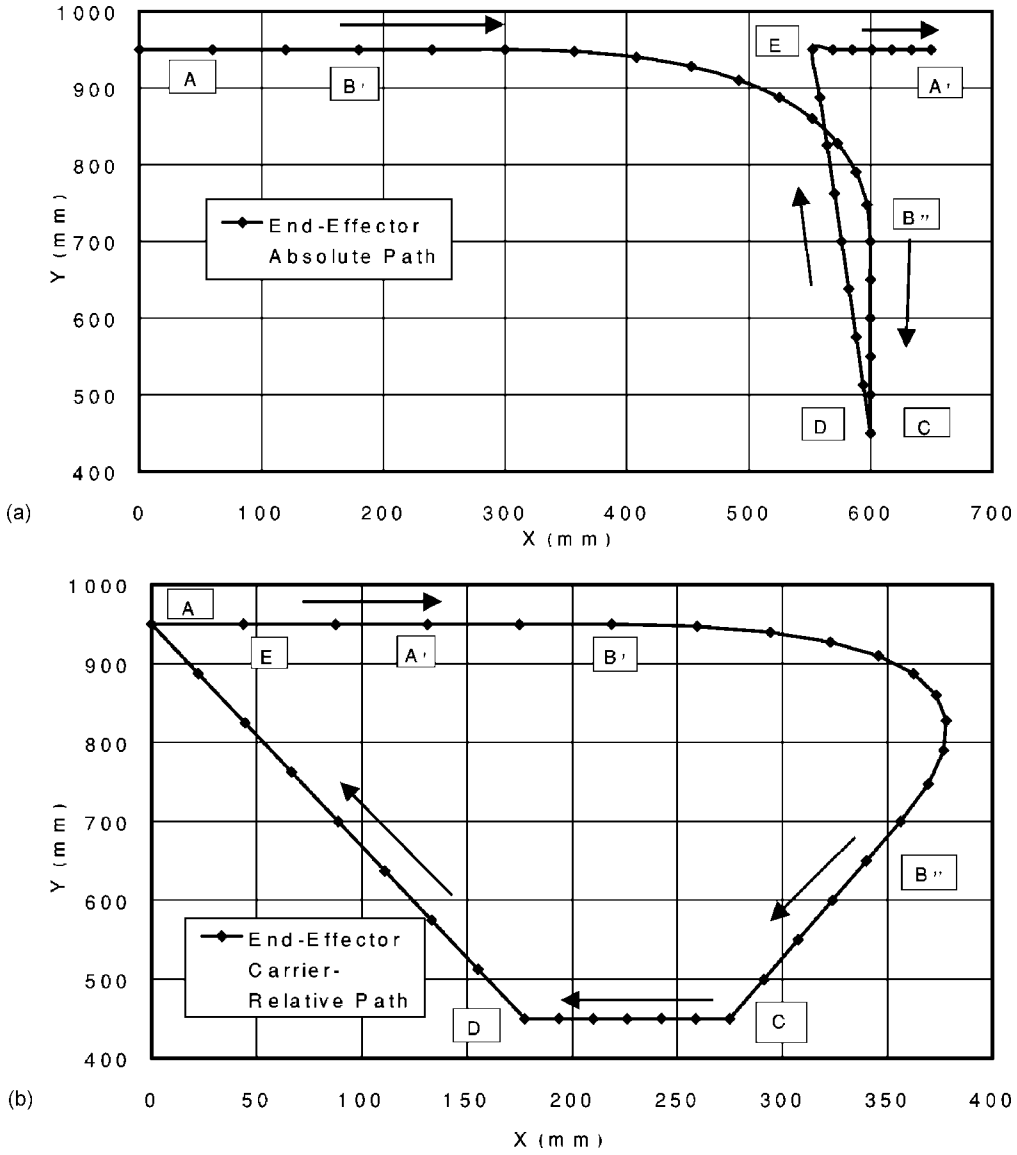

Figure 5. Harvesting cycle expressed in terms of path of the end-effector with respect to a ground frame (a), and to a carrier-embedded coordinate system (b).

(Figure 1), in order to avoid sudden waste and to ensure appropriate product storage. Also considering its high market value, radicchio lends itself very well to an automated harvesting process.

Details of the mechanical design of the two main components of the robot, i.e., the manipulator and the gripper, are discussed. The pneumatic muscle-actuated gripper is designed to satisfy the requirements for the harvesting of radicchio and the manipulator is geometrically optimized to gain a quasi-linear behavior and simplify the control strategy.

The robotic harvester autonomously performs its harvesting task using a vision-based module to detect and localize the plants in the field; we call the algorithm the *radicchio visual localization* (RVL). Visual measurements are as accurate as conventional measuring systems with the additional advantage of allowing contact-free estimations; they are critical to

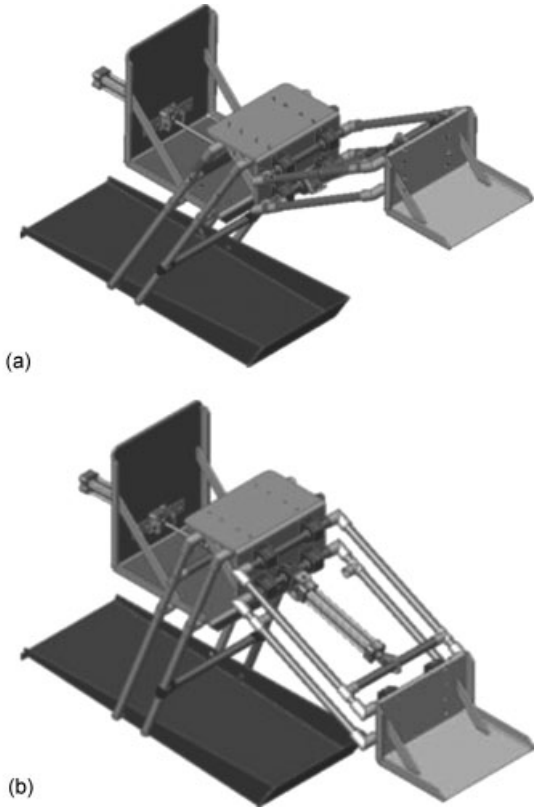

Figure 6. Mechanical design of the manipulator: Localization (a), and Harvesting (b) configurations.

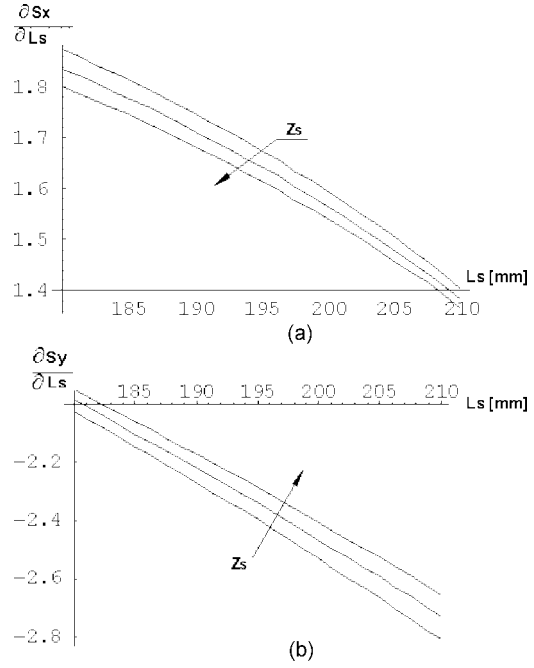

Figure 8. Variation of the shoulder position S with respect to its actuator stroke L_S. Rate-of-displacement along x direction (a), and y direction (b).

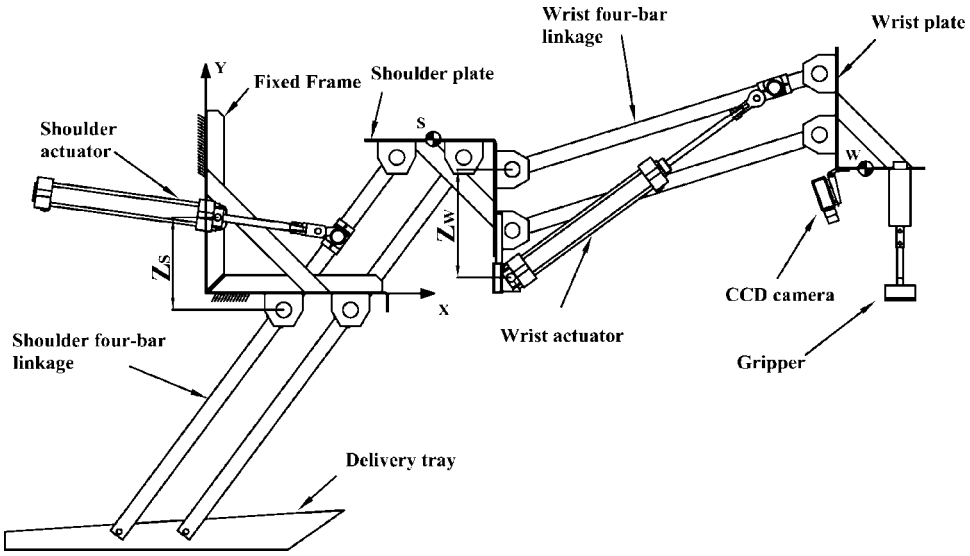

Figure 7. Manipulator nomenclature.

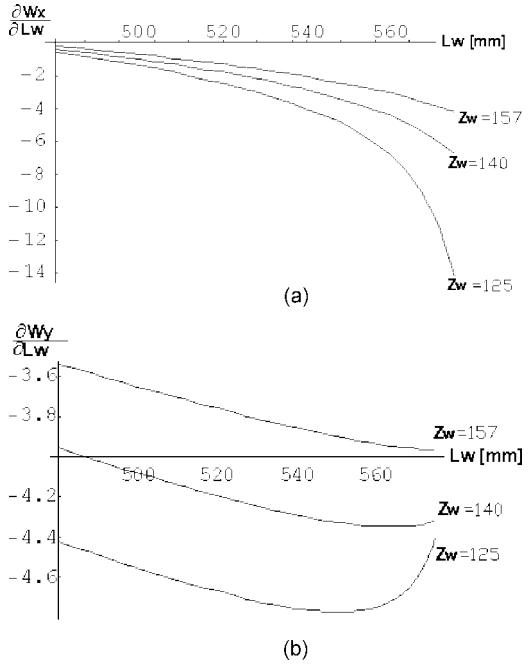

Figure 9. Variation of the shoulder plate position W with respect to its actuator stroke L_W. Rate-of-displacement along x direction (a), and y direction (b).

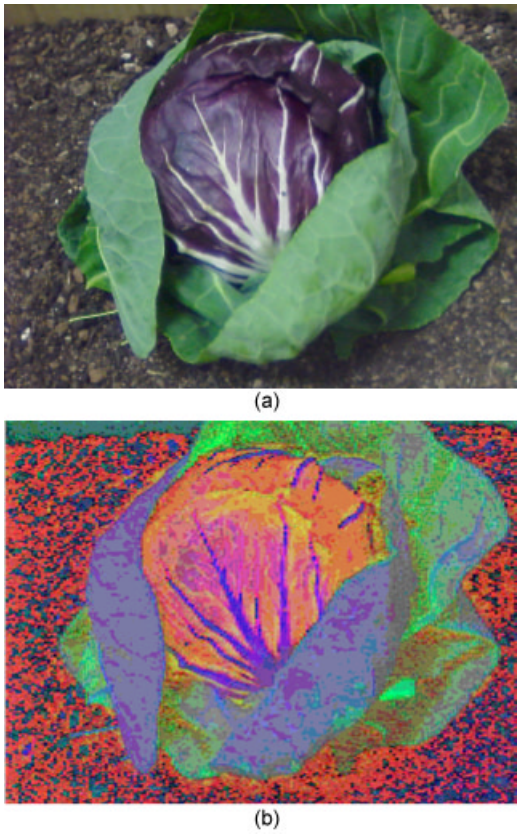

Figure 10. Sample image of the radicchio in the red, green, and blue (RGB) (a), and HSL (b) color spaces.

implement automated operations in agriculture (Chen, Chao, & Kim, 2002). Experimental results are presented, which were obtained with a prototype operating in a laboratory testbed to validate our approach and assess the performance and the robustness of the RVL. The vision-based module is also proven to be effective in tests in the field.

The paper is organized as follows. Section 2 presents the gripper and the manipulator. Sections 3 and 4 describe the RVL module and the control system, respectively. Finally, experimental results are discussed in Section 5 to show the feasibility of the system proposed.

2. MECHANICAL DESIGN

The robotic harvester was designed for both efficiency and cost effectiveness. It consists of a double four-bar manipulator and a gripper optimized for the harvesting of radicchio. Specifically, radicchio requires a stem cutting of the plant approximately 10 mm under the soil surface. Note that a radicchio plant is typically 120–130 mm in diameter with a 12 mm diameter stem.

Both the manipulator and gripper are pneumatically actuated. While pneumatic actuators are difficult to control, compared to electric actuators, they have a high power-weight ratio, which makes them suitable for agricultural applications. Furthermore, the gripper is designed to work with pneumatic muscles, which in turn are inexpensive, light, robust, and easy to maintain (Raparelli, Beomonte Zobel, & Durante, 2000). Pneumatic actuation also provides good compliance with the plant due to compressibility of air, which allows one to compensate for small errors in the measurement of radicchio position in the field (Kondo & Ting, 1998).

2.1. Gripper

All grasping devices should fulfill the following requirements: Low-cost, robustness, and simplicity in

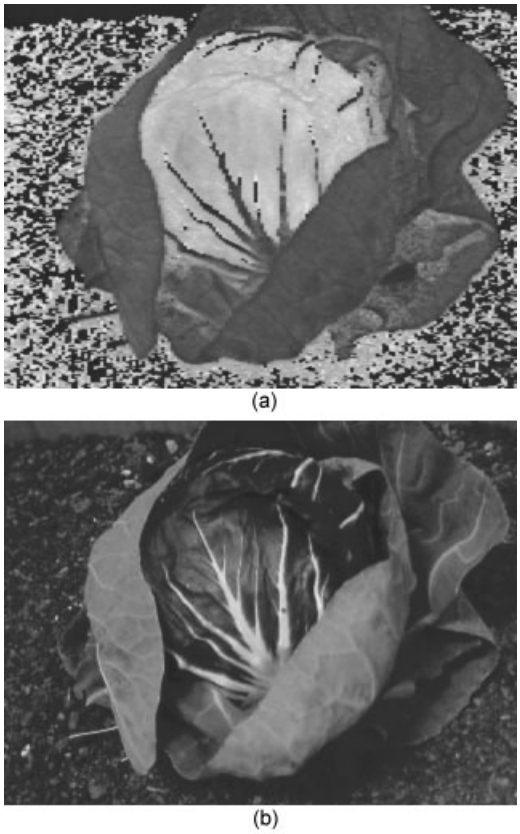

Figure 11. Hue (a), and luminance planes (b).

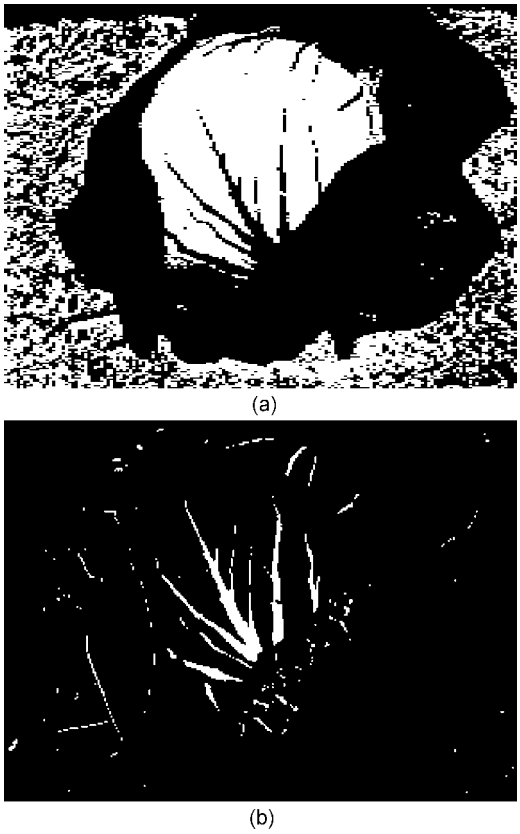

Figure 12. Thresholding in the hue (a), and luminance (b) planes.

the mechanical design, and easy implementation. Most robotic grippers are designed to operate with two fingers, since most of the grasps can be performed only with two fingers and two-finger grippers are the smallest suitable mechanical architectures for grasping hand devices (Ceccarelli, 2004).

Figure 2 shows the two-finger gripper prototype designed for our application; it is made of aluminum with an overall weight of approximately 16 kg, and employs two bucketlike fingers featuring a linear blade attached to their tips to perform the cutting operation. The driving linkage is actuated by two pneumatic muscles connected between the fixed plate F and the vertical slider S as indicated in Figures 2(a) and 2(b); the two fingers operate simultaneously with symmetrical behavior. Note that the vertical stroke a of the slider S, translates into a horizontal and vertical displacement of the fingertips denoted, respectively, with b and c in Figure 2(a). In the same figure, the fingertip paths are also shown by a dashed line.

The closure of the gripper starts when all four limit switches touch the soil [Figure 2(b)]. Afterward, the fingers cut the stem at about 10 mm underground and simultaneously pull the plant out of the terrain, as shown in Figure 2(c), by the successive configurations of the gripper during the whole operation. The relationship between the length of the pneumatic muscle and the displacement of the fingertip is shown in Figure 3.

2.2. Manipulator

The manipulator provides mobility to the gripper in order to approach the plant, perform the harvesting task, and deliver the radicchio to a container on the carrier. Requirements for the manipulator design are: The velocity of about 0.4 km/h of the carrier

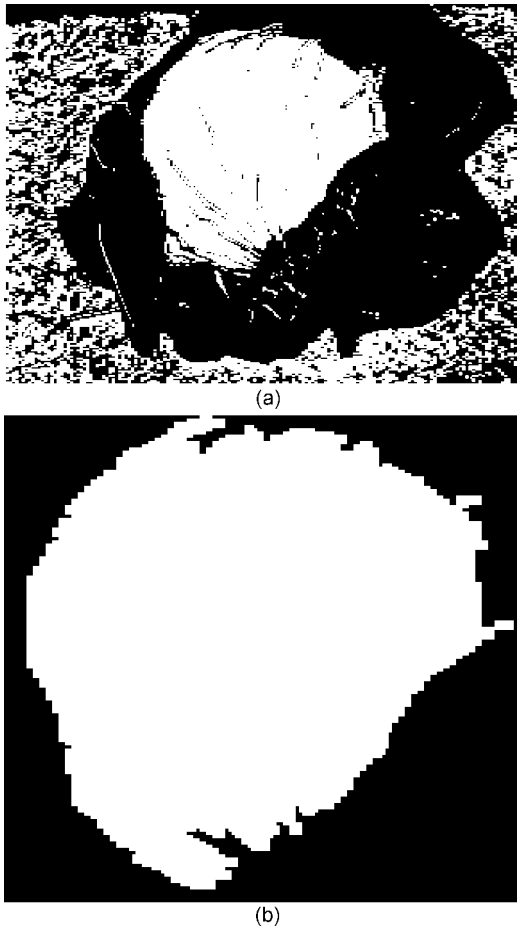

Figure 13. Or-operation between binary images (a), and morphological and particle filtering (b).

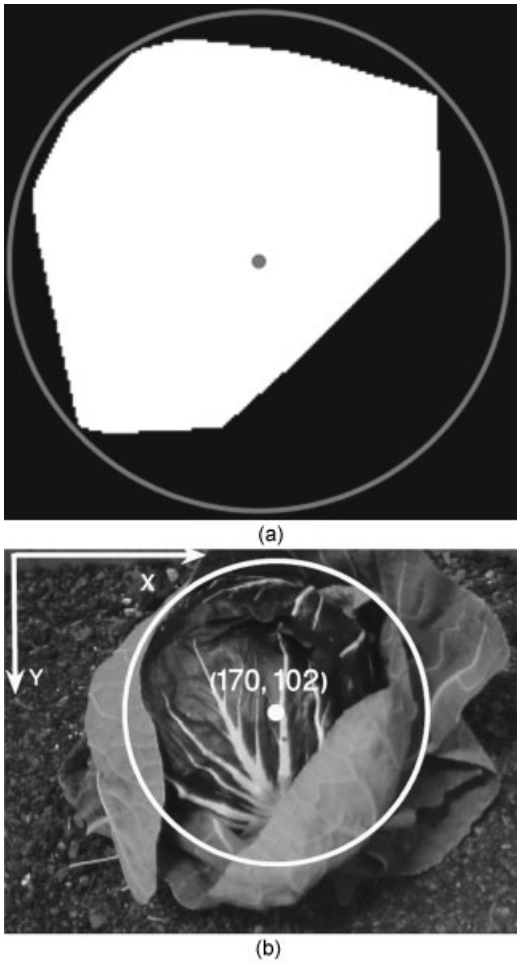

Figure 14. Convex hull and minimum enclosing circle generation (a), radicchio localization in the image plane (b).

(tractor) of the robotic harvester, the distance between the plants of about 700 mm along the field lines, and the minimum height of 800 mm from the ground that is required by the charge coupled device (CCD) camera attached to the gripper for an efficient identification of the plant in the field during the targeting stage.

The architecture of the manipulator is based on four-bar parallel links, which allow the gripper to stay level. Three candidate configurations are analyzed that utilize three, two, and one pneumatic actuators, respectively, as shown in the functional schemes collected in Figure 4. Note that in all solutions, a moving delivery tray is used to reduce the harvesting cycle time. Generally speaking, the number of actuated degrees of motions of a manipulator corresponds to the number of independent degrees of freedoms of the end-effector. The more degrees of motions, the higher the degree of flexibility and higher cost of the manipulator (Sciavicco & Siciliano, 2000). The one-actuator architecture [Figure 4(a)] would allow the lowest costs, but is less versatile; thus, the two-actuator configuration [Figure 4(b)] results in the best trade-off and has been chosen for our system.

Figure 5 shows a typical harvesting cycle path followed by the gripper with the two-actuator manipulator. The same path is referred to a ground reference frame in Figure 5(a), and to a coordinate system embedded with the carrier in Figure 5(b). The

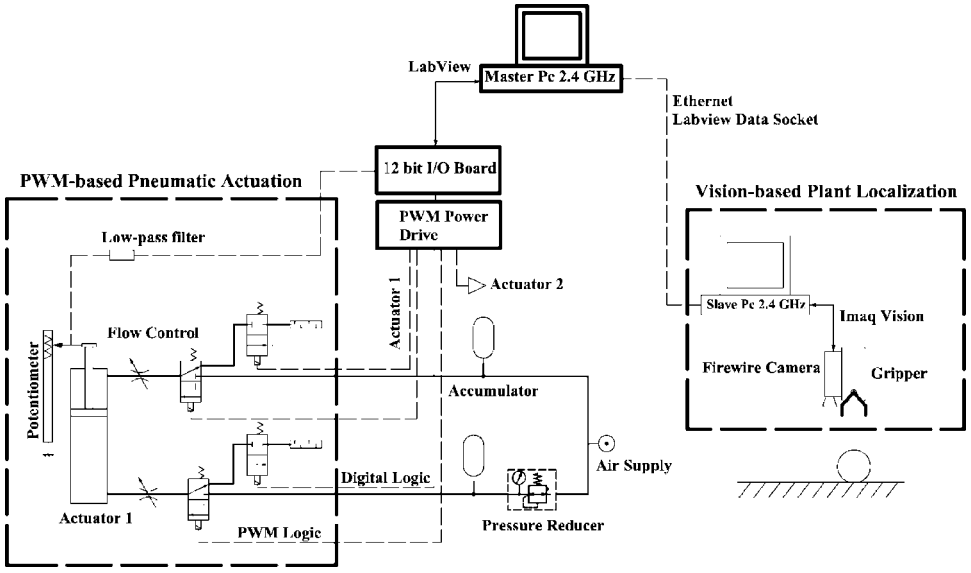

Figure 15. Control system block diagram.

gripper moves forward horizontally until the plant is localized by the vision-based module [point B' in Figures 5(a) and 5(b)]. Then, the gripper starts its downward course toward the plant (point C), where the gripper performs the cutting operation. Point D marks the return of the gripper toward the starting configuration where the plant is dropped on the delivery tray (point E) and the system can start the cycle again.

The mechanical design of the proposed manipulator is shown in Figure 6, where the "localization" and the "harvesting" configurations are shown. Note that in the practical implementation of the two-actuator manipulator, the shoulder prismatic joints have been replaced with a second four-bar mechanism, which provides a more economical and easy to maintain solution.

2.2.1. Geometrical Optimization

While the lengths of the links, the revolute joints, and the initial joint angles for the manipulator are set according to the workspace design data and economical considerations, the two linear actuators can be suitably fitted into the system with a geometrical optimization (Ceccarelli, 2004). The variables chosen for the optimization are, Z_S and Z_W, which are defined in Figure 7; Z_S identifies the position of the base joint of the shoulder actuator with respect to the fixed plate, and Z_W fixes the position of the base joint of the wrist actuator with respect to the shoulder plate. The objective is to find the appropriate values for Z_S and Z_W to establish a linear relationship between the strokes of the two actuators and the displacement of the shoulder and wrist plate of the manipulator, i.e., their representative points S and W, respectively (Figure 7). The idea is to develop a Cartesian robotlike behavior, which is very simple to control and suitable to be actuated by linear actuators.

The partial derivative of the shoulder position $S=[S_X S_Y]^T$, with respect to the shoulder actuator stroke L_S, is numerically obtained as function of L_S for different values of Z_S as reported in Figure 8. Similarly, the partial derivative of the wrist position $W=[W_X W_Y]^T$, with respect to the wrist actuator stroke L_W, is reported in Figure 9 as function of L_W for different values of Z_W. The optimization is developed considering only the movement of one actuator, while the other does not move.

The suboptimal set of values, which approximate the functions $(\partial S/\partial L_S)(L_S)$ and $(\partial W/\partial L_W)(L_W)$ to linear equations, results in: $Z_S=115$ mm and $Z_W=157$ mm.

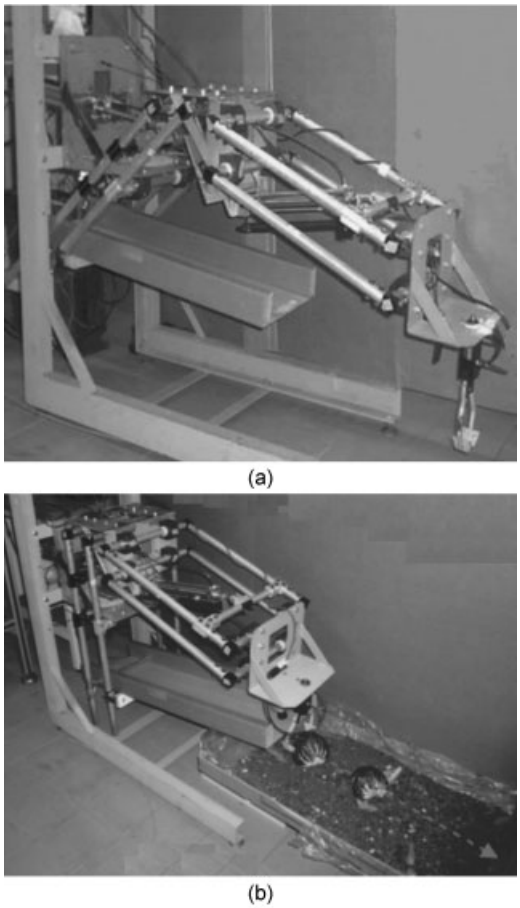

Figure 16. The robot arm prototype (a), and the laboratory testbed (b).

3. RADICCHIO VISUAL LOCALIZATION

A vision-based algorithm is developed with the aim of localizing the plants in the field; The RVL is based on intelligent color filters and morphological operations, which allow one to differentiate the radicchio within the images grabbed by a CCD color camera mounted on the wrist plate in a typical eye-in-hand application (Kondo & Ting, 1998).

Typically, the algorithm consists of the following steps:

1. Image acquisition in the hue saturation luminance (HSL) space in order to enhance the thresholding operation described below [Figure 10(b)].
2. Hue and luminance plane extraction in order to obtain two images, where the radicchio is visually distinct from the surrounding (Figure 11).
3. Independent thresholding in the hue and luminance planes in order to obtain two binary images comprising the radicchio purple pixels and white pixels, respectively (Figure 12). The thresholds are experimentally determined by analyzing the histogram of the two planes. Specifically, the threshold for the hue plane was found to be well defined as:

$$\frac{T_{\max} + T_{\min}}{2}, \tag{1}$$

where $T_{\max}$ and $T_{\min}$ are the maximum and minimum intensity values, respectively. The threshold for the luminance plane is set, instead, as the highest value of grey levels since the white parts of the plant correspond to the pixels with the largest luminance.
4. Or-operation of the two images in order to combine the information into a unique image [Figure 13(a)].
5. Morphological and particle filtering [Figure 13(b)]. Specifically, a morphological opening, i.e., an operation of erosion followed by dilation, is applied using a 5×5 pixel substructure to open up touching futures and remove isolated background pixels. Then, objects with an area, i.e., a total number of pixels, smaller than a threshold value (2000 pixels) are filtered out (Russ, 1994). Finally, a morphological closing, i.e., a succession of dilation and erosion, allows one to reconstruct the shape of the plant by bridging the remaining small gaps.
6. Convex hull generation of the extracted feature [Figure 14(a)].
7. Definition of the minimum enclosing circle [Figure 14(a)], i.e., the smallest circle which encloses the extracted set of points (Xu, Freund, & Sun, 2003). This geometrical algorithm helps to detect the plant even when only a relatively small uncentered portion of the radicchio is extracted, as demonstrated later in Section 5.2.

Figure 14(b) shows the overall result of the localiza-

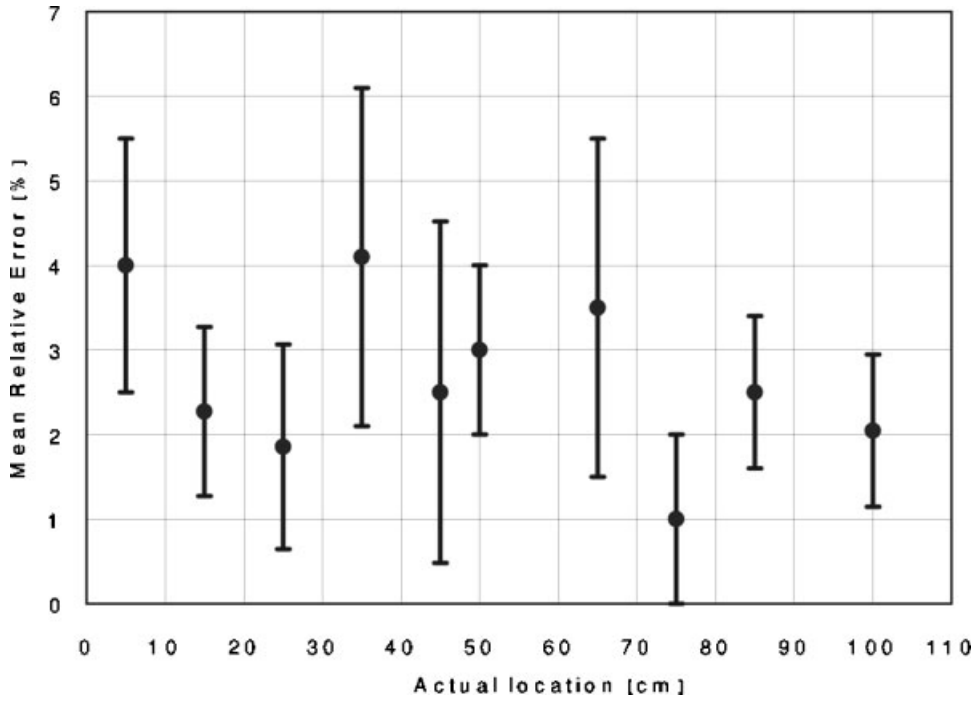

Figure 17. Error estimation for the RVL.

tion algorithm. The minimum enclosing circle is overlaid over the original image with its center indicating the coordinates of the centroid of the plant in the image reference frame.

4. CONTROL STRATEGY

The manipulator is actuated by two standard double-acting pneumatic cylinders. Both cylinders are driven by two three-way solenoid valves, and equipped with linear potentiometers for position feedback control (Figure 15). The system is position controlled using pulse-width modulation (PWM) (Gentile, Giannoccaro, & Reina, 2002), which allows for adopting on/off solenoid valves in place of more expensive and bulky servovalves; a CCD camera attached to the gripper provides plant identification and targeting.

Figure 15 shows the control system, which comprises a PWM-based actuation block and a vision-based targeting module. The two subsystems are governed by independent computers linked through an Ethernet connection.

Note that flow controls are added to the cylinder inlets to filter out the vibrations caused by the pulsing of the solenoid valves, and a manual pressure reducer is also added to balance the pull difference acting on the rod. The camera is a firewire Sony DFW, which takes 512 pixels $\times$ 480 pixels color images corresponding to field images of approximately 1.1 m $\times$ 0.7 m from a height of 1 m. All control codes are implemented in LABVIEW and IMAQVISION from National Instruments Corporation (2003). The plant visual identification starts processing when the end-effector is at its maximum height and the camera has the largest field of view. Once the radicchio is located, the "target" is set for the control system and the manipulator drives the gripper toward the plant follow-

Table I. Average time for a complete harvesting operation.

Operation	Time (s)
RVL	0.2
Plant approaching and harvesting	4.0
Plant delivering and arm reconfiguration	2.5

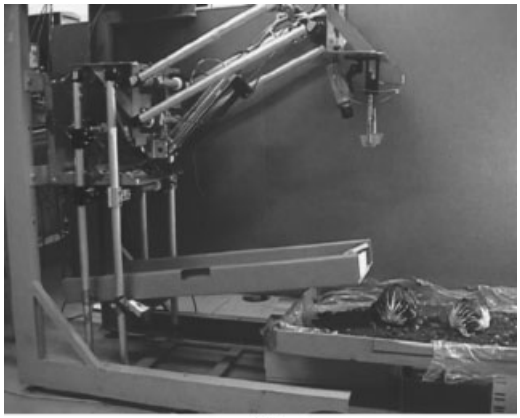

(a)

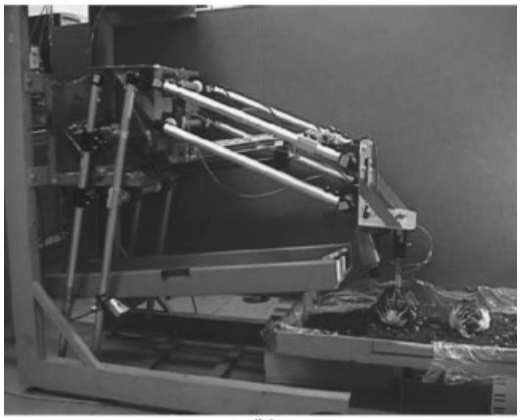

(b)

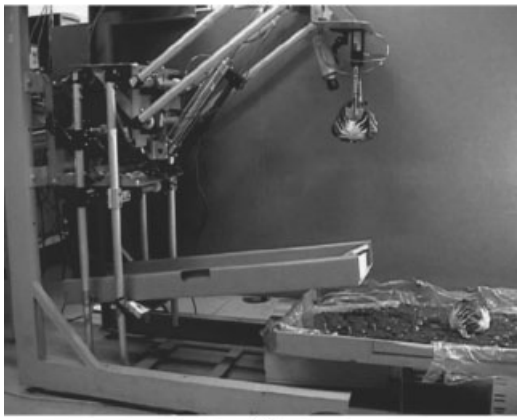

(c)

Figure 18. The robotic harvester during a test: Detection and targeting stage (a), harvesting stage (b), delivery stage (c).

ing its inverse kinematics. Note that during the end-effector's downward course, the RVL keeps tracking the targeted radicchio at a sampling rate of 200 ms, thus allowing one to compensate for a certain degree of positioning error of the gripper with respect to the plant due to unexpected speed variations of the carrier.

Figure 19. Influence of presence of rocks on the RVL performance.

5. EXPERIMENTAL RESULTS AND DISCUSSION

In this section, we present a feasibility study of the system performed through laboratory tests along with field validation of our vision-based module. The laboratory experiments are performed on a prototype operating in a testbed simulating quasi-real working conditions. This stage was helpful to set up and optimize the components of our system. Then, the performance of the RVL is validated in field tests. The prototype, shown in Figure 16, has three 3 mm thick steel plates to provide for the connection between the two four-bar linkages consisting of 20 mm diameter and 2 mm thick aluminum tubes, between the manipulator and carrier, and between the manipulator and gripper. All revolute joints are DryLin® bushings. A preliminary two-finger gripper was mounted at the end of the manipulator. The overall weight of the robotic arm is about 25 kg without the gripper. Figure 16(b) shows the laboratory testbed set with typical agricultural terrain and fist-size rocks spread across the test field.

5.1. Laboratory Tests

A set of experiments was performed to assess the performance of the robotic harvester in identifying and picking up radicchios that were randomly placed along the harvesting line [Figure 16(b)]. The plant position was derived by the RVL; a localization error E_j was defined for the measurement of the plant position j as:

$$E_j = \frac{1}{n}\sum_{i=1}^{1}\frac{|x_j - v_{j,i}|}{x_j}, \tag{2}$$

where n is the number of runs ($n=5$), x_j is the actual plant position measured by a ruler, and $v_{j,i}$ is the ith

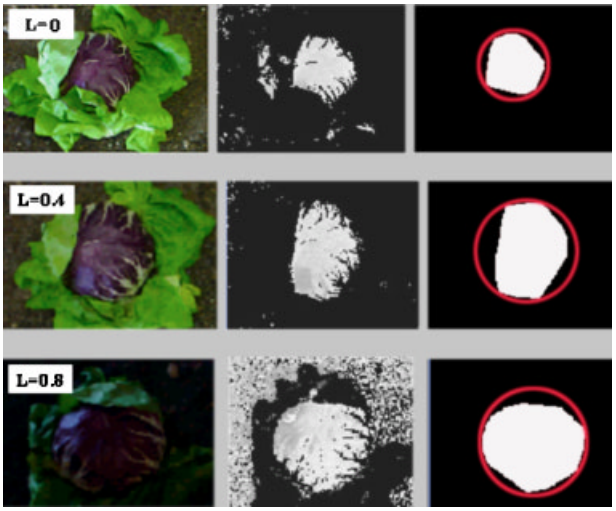

Figure 20. Lighting influence on the RVL.

vision-derived measurement. Ten different plant positions were analyzed along the 1 m long harvesting line using radicchios of various shapes and sizes; the results are presented in Figure 17, where E_j is reported along with the indication of its statistical spread.

The average error was always below 5% and, for the worst-case measurement, it was less than 6.3%. No false localization was detected, and no significant influence of the size and shape of the radicchio on the RVL performance was observed. In all experiments, the robotic harvester was consistently and successfully able to pick up the targeted plant. The average time for a complete harvesting operation was about 6.5 s, as indicated in detail in Table I. In Figure 18, an image sequence of the robotic harvester during operation is shown; the plant detection [Figure 18(a)], the harvesting [Figure 18(b)], and the delivery configuration [Figure 18(c)] are shown.

The sensitivity of the system to disturbances due to leaves and rocks was evaluated in laboratory tests. Figure 19 shows a sample image; proving the effectiveness of the RVL in presence of small rocks spread across the test field and leaves partially covering the plant. The algorithm was able to filter out all disturbances and detect correctly the radicchio.

The robustness of the algorithm to variations in lighting was also tested. Figure 20 shows the result of image segmentation under three different lighting conditions obtained by an adjustable video light. The RVL works very well even with a reduction of the environmental illumination level by as much as 80% of the optimal value ($L=0.8$), as shown in the bottom image set of Figure 20.

5.2. Field Tests

In this section, we present experimental results obtained in the field with our visual detection system. The RVL was extensively tested by performing several position estimation measurements in a field of radicchio ready for harvest on a cloudy day. Figure 21 shows a typical result for a plant recognition test. The RVL was able to correctly detect all six radicchio plants, with an error of always less than 5%. In all experiments, the actual distance was estimated with a portable laser distance measuring tool using the center of the plant as reference point. The radicchio, partially hidden by leaves (first plant of the lower row), was also detected accurately with an error of only 4.2%. The performance of the system was consistent with the laboratory results, but with better accuracy and robustness. No false detection was observed in the experiments. Note, however, that if the plant was completely obscured by leaves, it would not be possible to perform a correct image thresholding and the RVL would fail. In addition, the system would provide poor plant localization if the extracted part of the plant was too small and uncentered. However, these are very unlikely field conditions for a fully or almost fully germinated plant, and no such case was observed in the investigated radicchio field.

6. CONCLUSIONS

A robotic arm for the harvesting of red radicchio has been presented. Details of the functional and mechanical design of the manipulator and the gripper have been provided. The manipulator was based on double four-bar linkage and the gripper was optimized for fulfilling the requirement of accurately cutting the radicchio stem 10 mm underground. The whole design has been developed pursuing efficiency and cost effectiveness. Feedback control for the position and target of the radicchio in the field was provided by a gripper-embedded CCD color camera using an algorithm based on intelligent color filtering and morphological image operations.

The design requirements were based on an envis-

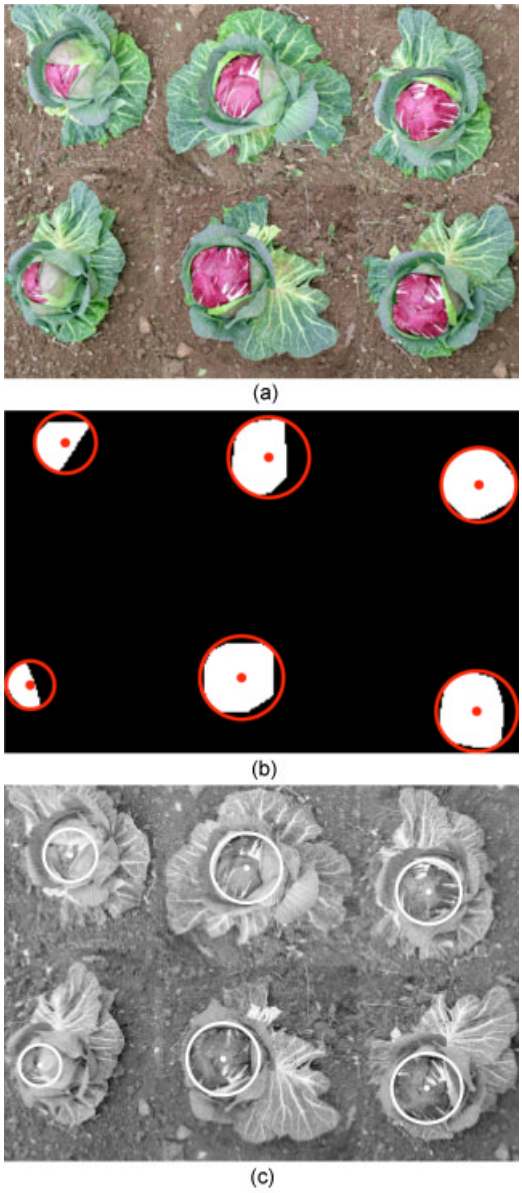

Figure 21. Plant detection in the field: Acquired image (a), plant thresholding (b), and radicchio localization (c).

aged tractor speed of about 0.4 km/h, a distance of 700 mm between radicchios, and a typical plant diameter of 150 mm. Thus, the required average cycle time was below 7 s. A feasibility study of the effectiveness of the system was presented by performing experimental tests on a prototype operating in a laboratory environment. The performance of the visual plant identification was also validated in the field. The robotic harvester successfully performed the harvesting task according to the design tolerances. The vision-based algorithm was able to correctly localize the radicchio plants with an average error within 5%, and showed time efficiency and robustness to disturbances due to rocks, leaves, and variations in lighting. It was shown that the robotic harvester could potentially be applied in the automated harvesting of high market value vegetables to improve quality and efficiency.

In the near future, the designed gripper will be mounted on the manipulator and the system will be employed in trials to test field performance of the whole system.

ACKNOWLEDGMENTS

The authors would like to express their gratitude to Annalisa Milella for the work on the vision-based algorithms. This work was funded by the Italian Department of Education, University and Research through a grant from *PRIN 2001*.

REFERENCES

Amaha, K., Shono, H., & Takakura, T. (1989). A harvesting robot of cucumber fruits. ASAE Paper No. 89-7053. St. Joseph, MI: ASAE.

Arima, S., Kondo, N., & Monta, M. (2004). Strawberry harvesting robot on table-top culture. ASAE Paper No. 04-3089. St. Joseph, MI: ASAE.

Åstrand, B., & Baerveldt, A. (2002). An agricultural mobile robot with vision-based perception for mechanical weed control. Auton. Rob., 13, 21–35.

Benson, E., Reid, J., & Zhang, Q. (2003). Machine vision-based guidance system for an agricultural small-grain harvester. Trans. ASAE, 46(4), 1255–1264.

Brown, G.K. (2002). Mechanical harvesting systems for the Florida citrus juice industry. ASAE Paper No. 02-1108. St. Joseph, MI: ASAE.

Burks, T., Villegas, F., Hannan, M., Flood, S., Sivaraman, B., Subramanian, V., & Sikes, J. (2005). Engineering and horticultural aspects of robotic fruit harvesting: Opportunities and constraints. HortTecnhology, 15(1), 79–87.

Cardenas-Weber, M., Hetzroni, A., & Miles, G.E. (1991). Machine vision to locate melons and guide robotic harvesting. ASAE Paper No. 91-7006. St. Joseph, MI: ASAE.

Ceccarelli, M. (2004). Fundamentals of mechanics of robotics manipulation. New York: Kluwer Academic.

Cerruto, E., & Schillaci, G. (1994). Algorithms for fruit detection in the citrus canopy. Paper presented at the

International Conference on Agricultural Engineering (*AGENG '94*), *Vol. I*, 128–136, Milano, Italy.

Chen, Y.R., Chao, K., & Kim, M.S. (2002). Machine vision technology for agricultural applications. Comput. Electron. Agric., 36, 173–191.

Chi, Y.T., & Ling, P., (2004). Fast fruit identification for robot tomato picker. ASAE Paper No. 04-3083. St. Joseph, MI: ASAE.

Dobrusin, Y., Edan, Y., Grinshpun, J., Peiper, U.M., & Hetzroni, A. (1992). Real-time image processing for robotic melon harvesting. ASAE Paper No. 92-3515. St. Joseph, MI: ASAE.

Doeney, D., Gilles, D.K., & Slaughter, D. (2003). Ground-based vision identification for weed mapping using DPGS. ASAE Paper No. 03-1005. St. Joseph, MI: ASAE.

Edan, T., Rogozin, D., Flash, T., & Miles, G.E. (2000). Robotic Melon Harvesting. IEEE Trans. on Robotics and Automation, 16(6), 831–834.

Gentile, A., Giannoccaro, N.I., & Reina, G. (2002). Experimental tests on position control of a pneumatic actuator using on/off solenoid valves. Paper presented at the International Conference on Industrial Technology (ICIT '02), Bangkok, Thailand.

Hannan, M.W., & Burks, T. (2004). Current developments in automated citrus harvesting. ASAE Paper No. 04-3087. St. Joseph, MI: ASAE.

Harrell, R.C., Adsit, R.D. Munilla, R.D., & Slaughter, D.C. (1990). The Florida robotic grove lab. Trans. of the ASAE, 33(2), 391–399.

Humburg, D.S., & Reid, J.F. (1992). Field performance of machine vision for the selective harvest of green asparagus. Trans. ASAE, 100(2), 81–92.

Jeon, H.Y., Tian, L.F., & Grift, T. (2005). Development of an individual weed treatment system using a robotic arm. ASAE Paper No. 05-1004. St. Joseph, MI: ASAE.

Kanemitsu, M., Yamamoto, K., Shibano, Y., Goto, Y., & Suzuki, M. (1993). Development of a Chinese cabbage harvester (Part 1). Japan Society of Agricultural Machinery, 55(5), 133–140.

Kawamura, N., & Namikawa, K. (1989). Robots in agriculture. Adv. Robo:. Robot. Soc. Japan, 3, 311–320.

Kondo, N., Monta, M., Shibano, Y., Mohri, K., Yamashita, J., & Fujiura, T. (1992). Agricultural robots (2): Manipulators and fruits harvesting hands. ASAE Paper No. 92-3518. St. Joseph, MI: ASAE.

Kondo, N., Nishitsuji, Y., Ling, P.P., & Ting, L.C. (1996). Visual feedback guided robotic cherry-tomato harvesting. Trans. ASAE, 39(6), 2331–2338.

Kondo, N., & Ting, K.C. (1998). Robotics for bioproduction systems. St. Joseph, MI. ASAE.

Ling, P., Ehsani, R., Ting, K.C., Chi, Y.-T., Ramalingam, M., Klingman, M., & Draper, C., (2004). Sensing and end-effector for a robotic tomato harvester. ASAE Paper No. 04-3088. St. Joseph, MI: ASAE.

Mattiazzo, G., Mauro, S., Raparelli, T., & Velardocchia, M. (1995). A fuzzy controlled pneumatic gripper for asparagus harvesting. Control Eng. Pract., 3(11), 1563–1570.

Monta, M., Kondo, N., Shibano, Y., Mohri, K., Yamashita, J., & Fujiura, T. (1992). Agricultural robots (3): Grape berry thinning hand. ASAE Paper No. 92-3519. St. Joseph, MI: ASAE.

Monta, M., Kondo, N., & Shibano, Y. (1995). Agricultural robot in grape production system. Paper presented at the IEEE Int. Conf. on Robotics and Automation, 2504–2509.

Monta, M., Kondo, N., & Ting, K.C. (1998). End-effector for tomato harvesting robot. Artif. Intell. Rev., 12, 11–25.

Murakami, N., Inoue, K., & Otsuka, K. (1995). Selective harvesting robot for cabbages. Paper presented at the Int. Symposium of Automation and Robotics in Bioproduction and Processing. Japan Society of Agricultural Machinery, 2, 24–31.

Nagata, M., & Cao, Q. (1998). Study on grade judgment of fruit vegetables using machine vision. Japan Agricultural Research Quarterly, 32 (4).

National Instruments Corporation. (2003). Advanced pattern matching concepts (IMAQ™).

Peterson, D.L., Whiting, M.D., & Wolford, S.D. (2003). Fresh-market quality tree fruit harvester. Part I: Sweet cherry. Applied Engineering in Agriculture, 19(5), 539–543.

Peterson, D.L. & Wolford, S.D. (2003). Fresh-market quality tree fruit harvester. Part II: Apples. Applied Engineering in Agriculture, 19(5), 545–548.

Pilarski, T., Happold, M., Pangels, H., Ollis, M., Fitzpatrick, K., & Stentz, A. (1999). The Demeter system for automated harvesting. Paper presented at the 8th Int. Topical Meeting on Robotics and Remote Systems, Pittsburgh, PA.

Raparelli, T., Beomonte Zobel, P., & Durante, F. (2000). On the design of pneumatic muscle actuators. Paper presented at the Internationales Fluidtechnisches Kolloquium, Vol. 2, 467–478, Dresda, Germania.

Russ, J.C. (1994). The image processing handbook. New York: CRC Press.

Sciavicco, L., & Siciliano, B. (2000). Modelling and control of robot manipulators. London: Springer.

Sitthichareonchai, A., & Sevila, F. (1989). A robot to harvest grapes. ASAE Paper No. 89-7074. St. Joseph, MI: ASAE.

Slaughter, M., & Harrel, R., (1987). Color vision in robotic fruit harvesting. Trans. ASAE, 30(4), 1144–1148.

Slaughter, M., Chen, P., & Curley, R.G. (1999). Vision guided precision cultivation. Precision Agriculture, 1, 199–216.

Van Henten, E.J., Hemming, J., Van Tuyl, B.A.J., Kornet, J.G., Meuleman, J., Bontsema, J., & Van Os, E.A. (2002). An autonomous robot for harvesting cucumbers in greenhouses. Auton. Rob., 13, 241–258.

Xu, S., Freund, R., & Sun, J. (2003). Solution methodologies for the smallest enclosing circle problem. Journal of Computational Optimization and Applications, 25, 283–292.